JOURNAL OF PROPULSION AND POWER
Vol. 23, No. 6, November–December 2007

Ignition and Oxidation of Lean CO/H_2 Fuel Blends in Air

Danielle M. Kalitan*
University of Central Florida, Orlando, Florida 32816-2450
John D. Mertens†
Trinity College, Hartford, Connecticut 06106
Mark W. Crofton‡
The Aerospace Corporation, El Segundo, California 90009
and
Eric L. Petersen§
University of Central Florida, Orlando, Florida 32816-2450

DOI: 10.2514/1.28123

Ignition and oxidation characteristics of CO/H_2 fuel blends were studied using both experimental and computer simulation methods. Shock-tube experiments were conducted behind reflected shock waves at intermediate temperatures ($890 < T < 1300$ K) for three pressure regimes of approximately 1, 2.5, and 15 atm. Results of this study provide the first undiluted fuel–air ignition-delay-time experiments to cover such a wide range of CO/H_2 composition (5–80% H_2) over the stated temperature range. Emission in the form of chemiluminescence from the hydroxyl radical (OH*)$A^2\Sigma^+ \rightarrow X^2\Pi$ transition near 307 nm was used to monitor the reaction progress from which ignition delay times were determined. In addition to the experimental analysis, chemical kinetics calculations were completed to compare several chemical kinetics mechanisms with the new experimental results. The models were in excellent agreement with the shock-tube data, especially at higher temperatures and lower pressures, yet there were some differences between the models at the higher pressures and lowest temperatures, in some cases by as much as a factor of 5. Ignition-delay-time and reaction-rate sensitivity analyses were completed at higher and lower temperatures and higher and lower pressures to identify the key reactions responsible for ignition. The results of the sensitivity analysis indicate that the ignition-enhancing reaction $H + O_2 = O + OH$ and hydrogen oxidation kinetics in general were most important, regardless of mixture composition, temperature, or pressure. However, lower-temperature, higher-pressure ignition-delay-time results indicate additional influence from HO_2- and CO-containing reactions, particularly, the well-known $H + O + M = HO_2 + M$ reaction and the $CO + O + M = CO_2 + M$ and $CO + HO_2 = CO_2 + OH$ reactions. Differences in the rates of the CO-related reactions are shown to be the cause of discrepancies among the various models at elevated pressures. Additional calculations were performed to show that the mixtures used are insensitive to small levels of water vapor, and the disagreement between experiment and model at the lowest temperatures and higher H_2 concentrations cannot be explained by possible impurities.

Introduction

IN RECENT years, the United States has developed an interest in establishing a hydrogen economy due, in large part, to the need for alternatives to hydrocarbon fuels. A candidate fuel for gas turbines and other power-generation and propulsion devices is synthesis gas, or syngas, that is produced during the coal gasification process. Syngas is mainly composed of CO and H_2, with minor amounts of N_2, CO_2, CH_4, and H_2O. Unlike common hydrocarbon fuels such as methane, propane, and kerosene, CO/H_2 oxidation arguably has not been well-characterized, especially for shock-tube and ignition-delay-time data. Hence, there is an increasing need for combustion chemistry data for CO/H_2 fuel combinations for a range of mixture compositions, temperatures, and pressures. Such data are especially critical because the implementation of syngas varies greatly throughout the world [1].

Early investigations of CO/H_2 oxidation sought to discover the reaction rates of CO/O_2 with minimal H_2 [2]. In particular, Sulzmann et al. [2] used a shock tube to examine the rapid formation of CO_2 during the induction period behind incident shock waves. Subsequently, additional shock-tube investigations were completed in a similar manner, and additional reaction rates were characterized for the $CO/H_2/O_2$ system [3–5]. After studying the exponential growth zone for nearly a decade, researchers turned to the study of the entire reaction history with the knowledge that reaction rates determined solely from induction-period data were seemingly incorrect [6]. Interest was again renewed in the $CO/H_2/O_2$ system when proper kinetics data were needed to validate simultaneous research of the kinetics of higher-order hydrocarbon systems [7,8]. During these experiments, data were collected over a range of temperatures to validate mechanisms for a broad range of experimental conditions. Simultaneously, kinetics modeling was applied to such systems and became another avenue to explore reaction rates and allowed for comparison of the theoretical results with experimental results [7,9–23].

In recent years, several new CO/H_2 kinetics mechanisms have been formulated [20–23]. With the addition of updated reaction rates, these new mechanisms are considerably more accurate than their predecessors. All four mechanisms, Davis et al. [20], Saxena and Williams, [21], Li et al. [22], and Sun et al. [23], used multiple experimental sources such as flame speed, flat flame, flow reactor, and shock-tube ignition data to optimize the reaction rates and provide a wide range of validity over which these mechanisms can be

---

Presented as Paper 3767 at the 41st AIAA/ASME/ASEE Joint propulsion Conference and Exhibit, Tucson, AZ, 10–13 July 2005; received 30 September 2006; revision received 1 June 2007; accepted for publication 23 July 2007.

*Research Assistant, Mechanical, Materials and Aerospace Engineering, P.O. Box 162450. Student Member AIAA.

†Associate Professor, Department of Engineering.

‡Senior Scientist, Space Materials Laboratory. Senior Member AIAA.

§Associate Professor, Mechanical, Materials and Aerospace Engineering, P.O. Box 162450. Senior Member AIAA (Corresponding Author).

used to predict experimental data. The results were improved mechanisms that describe the oxidation of CO and H_2 over a wider range of equivalence ratios, temperatures, and pressures.

Of most interest to the current study is the prediction of the aforementioned recent mechanisms to shock-tube ignition data. All of the mechanisms [20–23] have their kinetics calibrated to shock-tube data obtained from Dean et al. [7] with fairly good agreement. Two of the mechanisms [21,22] also used data from Gardiner et al. [5] and again were in good agreement. It should be noted, however, that the CO/H_2 mixtures used in both the Gardiner et al. [5] and Dean et al. [7] experiments were highly diluted in argon and conducted under conditions of relatively high temperatures: $1400 < T < 2500$ K and $1970 < T < 2745$ K for Gardiner et al. [5] and Dean et al. [7], respectively. Data obtained in this high-temperature region are known to possess different kinetic characteristics from those obtained for temperatures between 900 and 1300 K. In addition, both studies did not exceed pressures over 2 atm for the range of temperatures studied. Because the ignition characteristics of fuel/oxidizer mixtures can vary greatly depending on the shock-tube system parameters, it is desirable to understand how each of the four mechanisms compares to shock-tube data obtained for a wider range of CO/H_2 mixtures, temperatures, and pressures than previously studied. Therefore, to provide much needed ignition and oxidation data for the power-generation industry, new experimental data concerning ignition delay times must be compiled to compare results with the current CO/H_2 chemical kinetics mechanisms for validation and mechanism enhancement of regimes such as those encountered in gas-turbine and other power-generation environments.

This paper presents ignition-delay-time data for several different fuel-lean ($\phi = 0.5$) CO/H_2/air mixtures for temperatures between 890 and 1300 K and pressures ranging from 1 to 15 atm. Note that the mixtures investigated in the present study were undiluted fuel–air mixtures, in which shock-tube ignition data in the CO/H_2 system are scarce. The following sections of this paper include a discussion of the shock-tube facility used to conduct the CO/H_2/air fuel mixture experiments. Subsequently, the ignition-delay-time results are presented and compared with several current chemical kinetics mechanisms. In addition, the models are used to perform ignition-delay-time and reaction-rate sensitivity analyses to determine which reactions have the most effect on ignition times.

Experiment

Apparatus

All experiments were conducted using the shock-tube facility described by Petersen et al. [24]. This shock tube is constructed of stainless steel, and the tube's helium-driven driver section is 3.5 m in length and 7.62 cm in diameter. The driven section is 10.7 m in length with a 16.2-cm inner diameter. All experiments were performed behind the reflected shock wave, and reaction progress was monitored by emission from the hydroxyl radical $A^2\Sigma^+ \rightarrow X^2\Pi$ transition (i.e., OH* chemiluminescence). CaF_2 optical ports located on the endwall and sidewall of the shock tube allowed for nonintrusive optical access, and a Hamamatsu 1P21 photomultiplier tube (PMT) fitted with a narrow-band filter centered at 310 ± 5 nm collected the ultraviolet emission. A PCB 134A pressure transducer was located at the endwall, and five fast-response (less than 1 μs) PCB 113A pressure transducers and four Fluke model PM6666 time-interval counters monitored the incident shock speed at four different axial locations along the shock tube. The data acquisition system includes a Pentium computer and two CS512 computer oscilloscope boards from Gage Applied Sciences, which results in a total of four channels at a speed of 5 MHz per channel with 12-bit resolution. Further details of the shock-tube facility are reported elsewhere [24].

A complete list of all CO/H_2/air mixtures and OH* ignition-delay-time τ_{ign} data are provided in Tables 1 and 2, respectively. All mixtures were fuel-lean with a fuel–air equivalence ratio of $\phi = 0.5$ and premixed in tanks before being filled into the driven section of the shock tube. The air was theoretical air at the ratio of $O_2 + 3.76\,N_2$ using ultrahigh-purity N_2 and O_2. Figure 1 shows typical pressure and emission traces and defines ignition delay time as measured from the endwall location. The pressure signal indicated time zero, and the reaction profile was used to determine when ignition had occurred.

Ignition delay time τ_{ign} was measured from the endwall location and is defined in Fig. 1 using both the endwall pressure trace and the OH* emission trace. For all tests with weak to moderately strong ignition, the pressure signal indicated time zero, and ignition was indicated by the onset of the pressure increase due to combustion of the fuel mixture, which also coincided with the onset of OH* emission, as depicted in Fig. 1. Although endwall emission measurements for highly diluted mixtures lead to slightly longer ignition times due to the integrated effect of observing subsequent ignition events down the length of the tube, this effect is diminished in less-diluted mixtures such as those herein, because the ignition event tends to be rather abrupt and steplike in nature. Endwall emission (and pressure) measurements in undiluted mixtures are less susceptible to gas dynamic effects from the ignition event as opposed to sidewall measurements, which can appear accelerated. For a small number of test cases (namely, those at some of the lowest temperatures), extremely strong ignition and/or detonations were observed. For these strong ignition cases, ignition delay time was defined in terms of the endwall pressure spike, which can be seen in Fig. 2. It was also observed that these experiments, in most cases, displayed early and relatively significant OH* emission before the main ignition event at the endwall (Fig. 2).

Test temperatures behind the reflected shock wave were determined from the incident shock speed using the standard 1-D shock-tube relations and the Sandia National Laboratory's thermodynamic database [25]. The test temperature calculated in this way presents an uncertainty of less than 10 K for the facility used herein, as shown by Petersen et al. [24]. The precision in determining the ignition delay time is approximately 5 μs, and the overall uncertainty is within 10% of the τ_{ign} values provided herein, or about the width of a data symbol used to plot the data in the results section later.

Vibrational Relaxation

Typically in shock-tube experiments, the species behind the reflected shock wave are assumed to be in vibrational equilibrium. Because the present mixtures contain considerable levels of diatomic gases, the assumption of equilibrium thermodynamics must be verified. Of particular concern is the presence of large amounts of N_2 and CO, both notorious for their relatively slow vibrational relaxation times. The net result of finite vibrational relaxation times is potential uncertainty in the reflected shock temperature, which will be higher than the equilibrium temperature. The worst-case uncertainty in test temperature can be estimated by assuming frozen

Table 1 Mixtures employed in the present study

Mixture	Blend	X_{CO}	X_{H2}	X_{O2}	X_{N2}	T_{frozen} for given T_{equil}, K 900 K	 1250 K
1	20/80% CO/H_2	0.035	0.139	0.174	0.652	935	1340
2	40/60% CO/H_2	0.071	0.103	0.172	0.654	935	1341
3	60/40% CO/H_2	0.104	0.070	0.174	0.651	935	1342
4	80/20% CO/H_2	0.140	0.035	0.174	0.651	935	1343
5	90/10% CO/H_2	0.156	0.017	0.175	0.652	935	1345
6	95/5% CO/H_2	0.165	0.009	0.175	0.652	935	1347

Table 2 OH* ignition-delay-time data. Data in bold exhibited detonationlike ignition preceded by early OH* emission (with the exception of the points denoted by *, which only showed very strong ignition and no early emission.

Mixture	T, K	P, atm	τ_{ign}, μs
1	**916**	**1.1**	**2011**
	936	**1.1**	**1085**
	954	1.2	462
	957	1.1	311
	960	1.1	327
	972	1.1	191
	993	1.0	144
	994	1.1	181
	994	1.0	141
	1046	1.0	99
	1049	1.1	77
	1064	1.0	80
	1065	1.1	81
	1070	1.0	84
	1074	1.1	68
	1088	1.0	80
	1092	1.0	65
	1119	0.9	55
	1151	1.0	52
2	**914**	**1.1**	**2277**
	951	1.1	687
	996	1.1	181
	1036	1.1	111
	1072	1.1	87
	1125	1.1	67
	1175	1.0	55
	1187	1.0	39
	1241	1.0	29
3	**900**	**0.9**	**2935**
	933	**1.1**	**1471**
	948	1.1	600
	950	0.9	748
	1009	1.1	193
	1024	1.1	160
	1026	1.1	153
	1071	1.1	99
	1078	1.1	93
	1113	1.1	73
	1145	1.1	47
	1154	1.0	69
	1162	1.0	57
	1169	1.0	61
4	934	1.2	1427
	936	1.2	1331
	938	1.2	1015
	957	1.2	640
	976	1.2	337
	985	1.2	270
	987	1.1	268
	1015	1.1	219
	1024	1.1	173
	1046	1.1	139
	1061	1.1	131
	1100	1.1	96
	1156	1.1	83
	1183	1.1	63
	929	**2.6**	**2593**
	929	**2.5**	**1817**
	968	**2.5**	**1061**
	980	**2.6**	**978**
	992	**2.6**	**1015**
	1011	2.6	426
	1025	2.6	342
	1026	2.5	240
	1058	2.6	108
	1063	3.1	120
	1063	2.5	92
	1015	**13.7**	**2278**
	1080	**14.5**	**1153**
	1114	14.9	638

(continued)

Table 2 OH* ignition-delay-time data. Data in bold exhibited detonationlike ignition preceded by early OH* emission (with the exception of the points denoted by *, which only showed very strong ignition and no early emission. (Continued)

Mixture	T, K	P, atm	τ_{ign}, μs
	1139	14.9	364
	1182	17.9	136
	1190	16.8	82
5	960	1.2	1307
	964	1.2	1067
	1012	1.2	420
	1033	1.1	289
	1041	1.1	316
	1052	1.1	274
	1087	1.1	202
	1125	1.1	154
	1157	1.1	116
	1197	1.1	101
	981	**2.7**	**2284**
	991	**2.6**	**994**
	1016	2.6	582
	1018	2.2	497
	1026	2.6	434
	1048	2.5	236
	1060	2.1	166
	1076	2.5	143
	1088	2.5	132
	1112	2.1	90
	1118	2.5	94
	1148	2.3	70
	1063	**14.3**	**1695**[a]
	1090	13.6	842
	1117	13.3	644
	1123	15.2	546
	1126	11.9	472
	1139	14.3	395
	1158	14.7	272
	1159	13.2	265
	1221	15.7	72
	1265	17.1	25
6	968	1.2	1365
	977	1.2	1099
	979	1.2	856
	982	1.1	970
	1010	1.2	611
	1034	1.1	399
	1050	1.1	272
	1051	1.2	282
	1057	1.1	297
	1090	1.1	229
	1108	1.1	246
	1110	1.1	222
	1126	1.1	170
	1145	1.1	146
	1176	1.0	129
	1195	1.1	99
	1206	1.0	112
	1263	1.1	82
	977	2.3	1538
	1005	2.3	1005
	1010	2.2	780
	1034	2.2	453
	1039	2.1	363
	1085	2.1	191
	1114	2.1	139
	1149	2.0	114
	1167	2.0	87
	1181	1.9	77
	1230	1.9	70
	1285	1.9	55
	1304	1.7	51
	1074	**19.2**	**1823**[a]
	1110	**12.7**	**1186**[a]
	1114	14.6	813
	1121	14.0	758

(continued)

Table 2 OH* ignition-delay-time data. Data in bold exhibited detonationlike ignition preceded by early OH* emission (with the exception of the points denoted by *, which only showed very strong ignition and no early emission. (Continued)

Mixture	T, K	P, atm	τ_{ign}, μs
	1142	13.6	713
	1144	14.8	748
	1151	13.9	435
	1163	13.5	266

[a]Strong ignition only.

vibrational energy between the driven-gas fill conditions and the reflected shock conditions. Table 1 contains the calculated frozen temperatures for each mixture at the extremes of target equilibrium temperatures of 900 and 1250 K. For a target of 900 K, the highest the temperature can be, due to nonequilibrium vibrational energy, is 935 K, or a 35-K difference between the equilibrium and frozen temperatures. The difference is higher at the higher test temperature of 1250 K, which can have a 1347-K frozen temperature, or a 103-K difference.

Fortunately, the time that it takes the molecules in the test gas to vibrationally relax can be estimated. Various theories are available for the vibrational relaxation time τ_v, the most-used theory for collisions between two molecules being [26]

$$\tau_v \approx C\frac{\exp(A/T^{1/3})}{P} \tag{1}$$

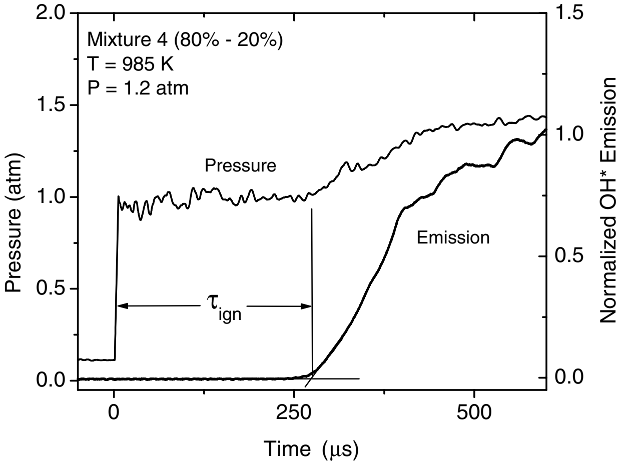

Fig. 1 Definition of ignition delay time τ_{ign} for mixture 4.

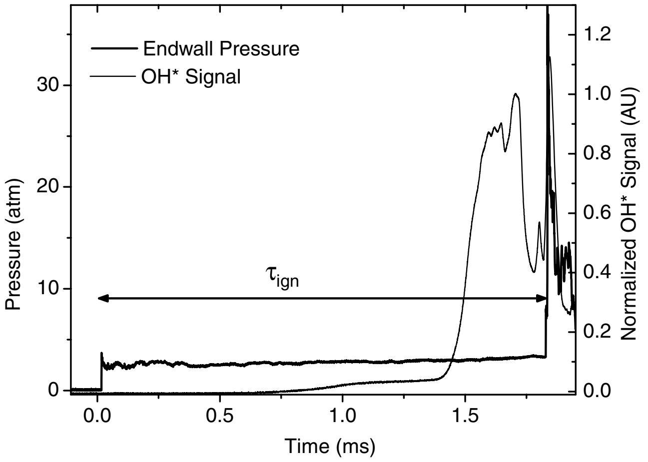

Fig. 2 Definition of ignition delay time τ_{ign} for strong ignition and detonations, taken from mixture 4 (80/20 CO/H_2), 929 K, 2.5 atm.

Table 3 Empirical constants for vibrational relaxation calculations

Colliders	A	C	Source
N_2-N_2	220	1.69×10^{-5}	[24]
CO-N_2[a]	220	1.69×10^{-5}	[27,28]
CO-N_2	68	3.10×10^{-3}	[24]
O_2-N_2	124	2.43×10^{-4}	[25]
O_2-O_2	129	2.09×10^{-4}	[24]
O_2-H_2	42	4.78×10^{-3}	[24]
H_2-H_2	80	2.06×10^{-3}	[26]
CO-CO	175	6.24×10^{-5}	[24]

[a]Assumed to be the same as N_2-N_2 per cited references.

Table 4 Vibrational relaxation times for each species in the six mixtures for representative test temperatures of 900 and 1250 K (at 1 atm)

	τ_v for 900 and 1250 K, μs			
Mixture	CO	H_2	O_2	N_2
1	26, 12	0.4, 0.3	3, 2	3, 2
2	35, 17	0.4, 0.3	4, 2	4, 2
3	51, 25	0.4, 0.3	5, 3	5, 3
4	103, 49	0.4, 0.3	10, 6	11, 6
5	210, 99	0.4, 0.3	19, 10	21, 13
6	394, 183	0.4, 0.3	31, 14	39, 22

where τ_v is in microseconds; C, and A are constants; T is the equilibrium temperature in Kelvin; and P is the pressure in standard atmosphere. When estimating the vibrational relaxation time for a mixture of molecules, the effect of each colliding pair can be taken into account via the relation presented by Millikan and White [27]:

$$\frac{1}{\tau_{v,A}} = \frac{X_A}{\tau_{v,A-A}} + \sum_i \frac{X_{B,i}}{\tau_{v,A-B_i}} \tag{2}$$

where $\tau_{v,A}$ is the overall vibrational relaxation time for species A in microseconds; X_A is the mole fraction of species A; $X_{B,i}$ is the mole fraction of the collider species B; $\tau_{v,A-A}$ is the vibrational relaxation time from binary collisions between species A; and $\tau_{v,A-B_i}$ are the vibrational relaxation times for binary collisions between species A and B_i. For example, the overall relaxation time for CO molecules in the mixtures herein (Table 1) involving CO, H_2, O_2, and N_2 would be written as

$$\frac{1}{\tau_{v,\mathrm{CO}}} = \frac{X_{\mathrm{CO}}}{\tau_{v,\mathrm{CO-CO}}} + \frac{X_{\mathrm{H_2}}}{\tau_{v,\mathrm{CO-H_2}}} + \frac{X_{\mathrm{O_2}}}{\tau_{v,\mathrm{CO-O_2}}} + \frac{X_{\mathrm{N_2}}}{\tau_{v,\mathrm{CO-N_2}}} \tag{3}$$

Similar relations can be written for the relaxation times for H_2, O_2, and N_2.

Using the preceding procedure, the vibrational relaxation times for the species at conditions representative of those herein (i.e., 1 atm and the two extreme temperatures 900 and 1250 K) were calculated. The constants A and C from Eq. (1) are well known and were obtained from the literature. Table 3 presents the constants used herein, taken from Millikan and White [27], White and Millikan [28], Dove and Teitelbaum [29], Hooker and Millikan [30], and Millikan and White [31]. Not shown in Table 3 is the N_2-H_2 combination, which was assumed to have the same relaxation parameters as O_2-H_2. The results for the present six mixtures are provided in Table 4. As expected from observations in the literature, hydrogen molecules tend to speed up the relaxation process considerably, and this phenomenon is evident in the calculated results in Table 4 that show decreasing τ_v for increasing H_2 presence.

For both extremes in temperature (i.e., 900 and 1250 K), hydrogen molecules should relax in less than 1 μs for all mixtures. However, the key species in terms of its effect on the mixture temperature is nitrogen, because it is present at the greatest levels. Nitrogen is shown in Table 4 to relax within 3 μs at 900 K for the mixture with the most hydrogen (mixture 1) and within 39 μs at 900 K for the mixture with the least amount of H_2 (mixture 6). Because the lowest τ_{ign} time for mixture 6 is only 82 μs (Table 2), vibrational relaxation of N_2 is not expected to be a problem herein, particularly, when the majority of ignition times for this mixture are much greater than 100 μs. Similar comments can be made for the relaxation times of the oxygen molecules, which are similar to those of N_2 (Table 4). Based on the frozen temperature of 935 K for the worst-case scenario of slowest relaxation (Table 1), the maximum uncertainty in average temperature due to vibrational relaxation would be approximately 15 K during the first 39 μs of an ignition event for mixture 6. The uncertainty would be much less at higher temperatures and for the mixtures containing greater levels of hydrogen.

In contrast, the carbon monoxide molecules at 900 K can have relaxation times ranging from 26 to 393 μs, depending on H_2 content. At 1250 K, estimated CO relaxation times range from 12 to 181 μs. For the shortest ignition times, the vibrational relaxation time can be a noticeable percentage of the prereaction time. However, because the levels of CO in each mixture are less than 20% by volume, the impact of nonequilibrium CO molecules on the test temperature is slight and less than 5 K at the extreme cases. The impact of nonequilibrium CO on the chemical kinetics is also assumed herein to be negligible (in light of the discussion later), although this behavior was not incorporated into the chemical kinetics calculations presented herein.

Interestingly, it should be pointed out that according to Millikan and White [31], the near resonance of the CO and N_2 vibrational energy levels led to CO relaxation times being nearly identical to N_2 relaxation times in their experiments involving mixtures of CO highly diluted in N_2. This behavior does not show up when using Eq. (3) to determine $\tau_{v,\mathrm{CO}}$; whether $\tau_{v,\mathrm{CO}}$ would be the same as $\tau_{v,N2}$ in syngas–air mixtures is perhaps a subject for further study. If this synchronization of vibrational relaxation times did occur in syngas–air mixtures, then the times for CO vibrational relaxation presented in Table 4 are much too long and would be closer to those of nitrogen. Also, we have considered herein only V-T processes and neglected V-V processes. We feel that this provides a conservative estimate, because additional V-V processes would only speed up the vibrational relaxation time. The end result would be the same; that is, the relaxation times are not long enough to significantly affect the present results.

Results and Analysis

Contained in the following sections are several types of analyses. The first compares ignition-delay-time data obtained in this study with those predicted by five different chemical kinetics mechanisms. The second includes an ignition-delay-time sensitivity analysis that determined which reactions have the largest influence on ignition for lower (900 K), intermediate (1050 K), and higher (1250 K) temperatures, as well as at lower (~1 atm), intermediate (~2.5 atm), and higher pressures (~15 atm). The third is a reaction-rate sensitivity analysis performed for several key radicals to determine their relative importance corresponding to the onset of ignition.

Ignition-Delay-Time Data

As mentioned previously, experimental data were collected for a wide range of reflected shock temperatures (890 K < T < 1300 K) with pressures ranging from 1 to 15 atmospheres for the mixtures listed in Table 1. Although data were collected at 1 atm for all six mixtures, intermediate (~2.5 atm) and high (~15 atm) pressure data were only collected for mixtures 4–6. As the hydrogen content of the mixture increased, it became exceedingly more difficult to obtain the ignition-delay-time data due to the propensity of the mixture to ignite behind the incident shock wave. Therefore, for mixtures containing more than 40% hydrogen, only 1-atm data were obtained. For the model comparison, each of the five mechanisms mentioned earlier was employed using the same mixture compositions, temperatures, and average pressures as the experimental conditions; however, OH was used to indicate when ignition had occurred. For such high-concentration exothermic mixtures, it is not necessary to add an OH* mechanism, such as in Hall and Petersen [32], to the models mentioned earlier, because the induction times obtained from OH and OH* (and most other species) are identical. Hence, ignition from either OH or OH* is indistinguishable as defined herein when obtained from the chemical kinetics model. Figures 3–11 display the results of this analysis on Arrhenius plots, along with the experimental data.

It is evident from Figs. 3–11 that all five mechanisms, Davis et al. [20], Saxena and Williams [21], Li et al. [22], Sun et al. [23], and GRI-Mech 3.0 [33], hereafter referred to as the Davis, San Diego, Li, Sun, and GRI mechanisms, respectively, accurately model the oxidation of CO/H_2 combustion for higher temperatures (greater than 1000 K) and low to high pressures (1 < P < 15 atm). Within these pressure regimes, the lower-temperature experimental data (less than 1000 K) are more accurately modeled by the Davis and San Diego mechanisms than the other three mechanisms. The GRI mechanism [33] is perhaps the least effective at modeling the behavior of CO/H_2 oxidation, although it nonetheless captures the primary temperature trends. This result is also not unexpected, because GRI-Mech 3.0 was designed for higher-temperature oxidation and is largely a methane-oxidation mechanism. Also, in the low- to intermediate-pressure range (1–3 atm), all five mechanisms model the shift in temperature dependence between 1100 and 1000 K quite well. This shift in temperature dependence is due to the well-known chain-termination kinetics near the second explosion limit of the hydrogen system, as described more fully later.

At higher pressures (~15 atm), as shown in Figs. 6–8, there is some disagreement between each of the models, although the general behavior of the data is represented well. Although the models have a tendency to disagree with one another, there tends to be agreement

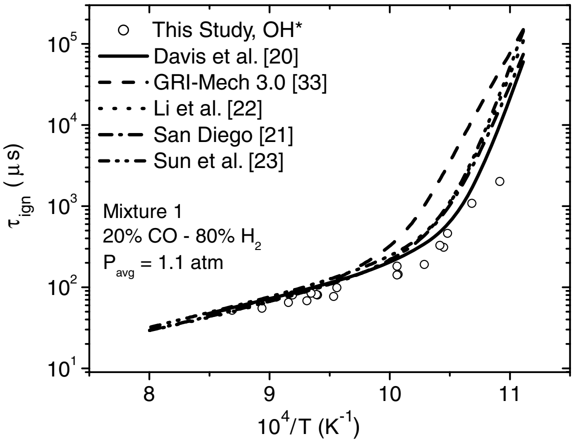

Fig. 3 Ignition-delay-time data and model comparison for mixture 1.

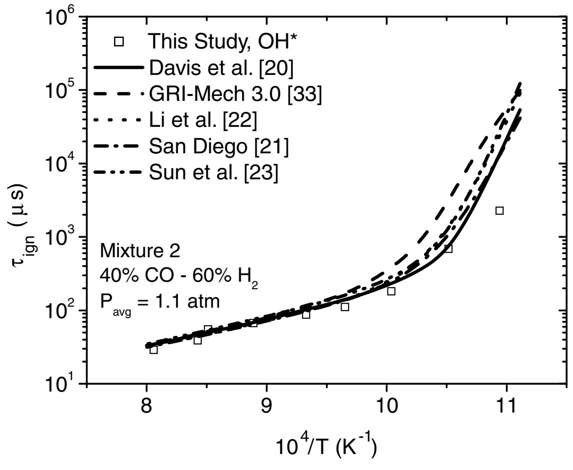

Fig. 4 Ignition-delay-time data and model comparison for mixture 2.

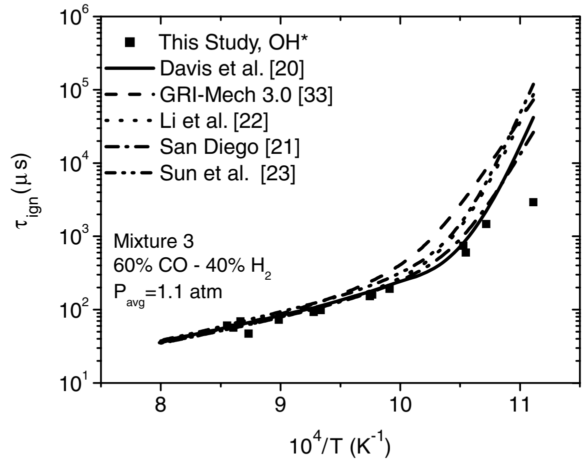

Fig. 5 Ignition-delay-time data and model comparison for mixture 3. As exemplified in this figure and those shown previously, the Davis et al. [20] and San Diego mechanisms [21] are consistently in good agreement with the experimental data.

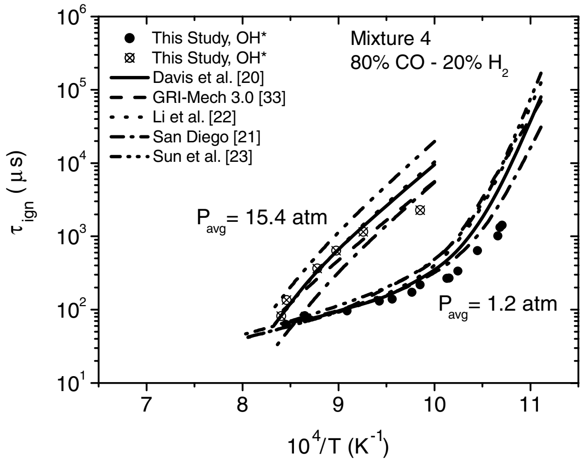

Fig. 6 Ignition-delay-time data and model comparison for mixture 4. The models show less agreement with one another in the high-pressure regime than in the low-pressure case.

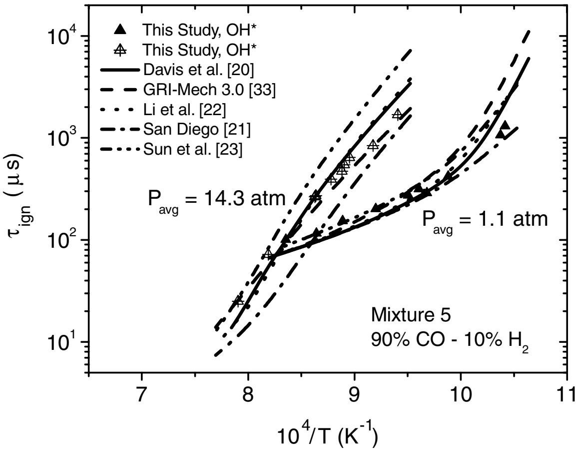

Fig. 7 Ignition-delay-time data and model comparison for mixture 5. Here, the San Diego mechanism [21] accurately predicts the behavior of the data over the entire temperature range for the low-pressure data.

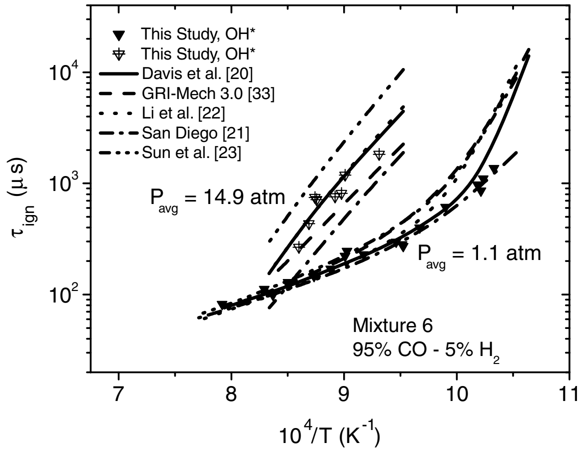

Fig. 8 Ignition-delay-time data and model comparison for mixture 6. The San Diego mechanism [21] most accurately predicts the low-pressure data over the entire temperature range. In the high-pressure regime, there is less agreement between the models.

with particular models and the data within specific temperature ranges. For example, the Li and Davis mechanisms show good agreement with mixture-4 experimental data at high temperatures (Fig. 6), whereas the GRI and San Diego mechanisms predict the ignition trend of mixture 4 with more accuracy at lower temperatures. The varied behavior of the models at higher pressures is not surprising considering the lack of existing CO/H_2 data for this pressure regime. It should be noted here that the San Diego mechanism is noticeably more accurate than the other four mechanisms for mixtures 5 and 6 (Figs. 7, 8, 10, and 11) between 1 and 3 atm. For these mixtures specifically, the San Diego mechanism models the low-temperature data extremely well, whereas all the other mechanisms show deviations of a factor of 2 or more from the experimental data.

Although all five mechanisms capture the change in activation energy from low to high temperatures between 1 and 3 atm, Figs. 3, 4, 6, and 9 all show the models' tendencies to overpredict some of the experimental data at temperatures below approximately 1000 K. However, upon closer inspection, these lowest-temperature data points were all observed to have ignition behavior that differed from all the other points. That is, the points shown in bold in Table 2 all displayed prominent OH* emission before the main ignition event (as seen from the endwall trace in Fig. 2); also, the main ignition event in these data occurred rather abruptly with not only very strong ignition behavior, but behavior approaching the characteristics of a detonation wave with pressure ratios on the order of 10 or higher. The relatively early OH* emission as seen from the endwall port may be an indication of nonhomogeneous combustion in regions removed from the endwall. Curiously, no accompanying pressure increase was seen before the main ignition event. Although the cause of this sudden transition from well-behaved ignition at slightly higher temperatures to extreme and seemingly early ignition at slightly lower temperatures is not known at this time, there is a clear correlation between the few lowest-temperature points showing fast ignition and the extreme gas dynamic coupling. Further discussion on this phenomenon is presented in later sections.

To better understand the oxidation and ignition of CO/H_2 for both high- and low-temperature and high- and low-pressure regimes in the future, ignition-delay-time and reaction-rate sensitivity analyses were conducted to learn which reactions are most dominant at higher (1250 K), intermediate (1050 K), and lower (900 K) temperatures, as well as at high and low pressures. These sensitivity analyses are presented in the following section.

Sensitivity Analysis

Using the Shock module in the Chemkin Collection [34] software package, an ignition-delay-time sensitivity analysis was conducted for mixture 1 (20% CO and 80% H_2) and mixture 6 (95% CO and 5% H_2) for both lower (900 K) and higher (1250 K) temperatures at 1 atm using the Davis mechanism. Mixtures 1 and 6 were chosen for analysis based on their mixture composition. It was deemed

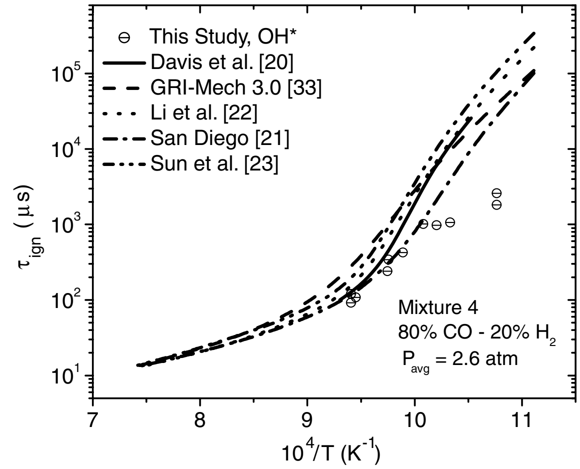

Fig. 9 Ignition-delay-time data and model comparison for mixture 4. All five models exhibit increasingly larger ignition delay times at lower temperatures; however, the experimental data do not demonstrate such a rapid increase in ignition delay time.

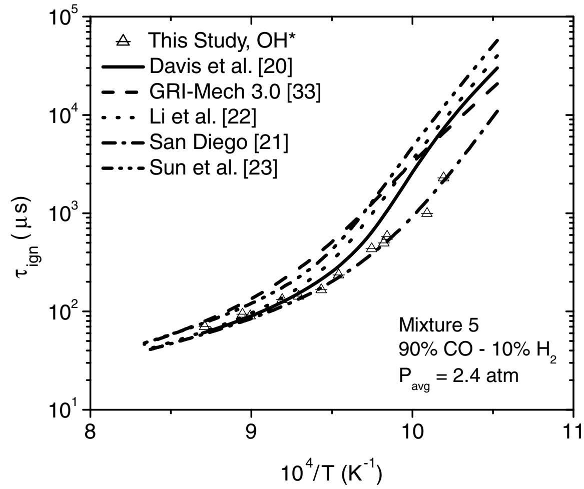

Fig. 10 Ignition-delay-time data and model comparison for mixture 5. The San Diego mechanism [21] predicts the behavior of the experimental data most accurately.

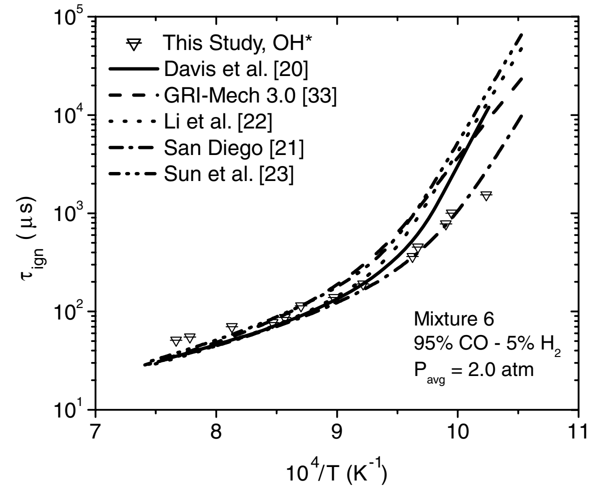

Fig. 11 Ignition-delay-time data and model comparison for mixture 6. Similarly to mixture 5 (∼2 atm), the San Diego mechanism [21] most accurately predicts the ignition delay time for mixture 6.

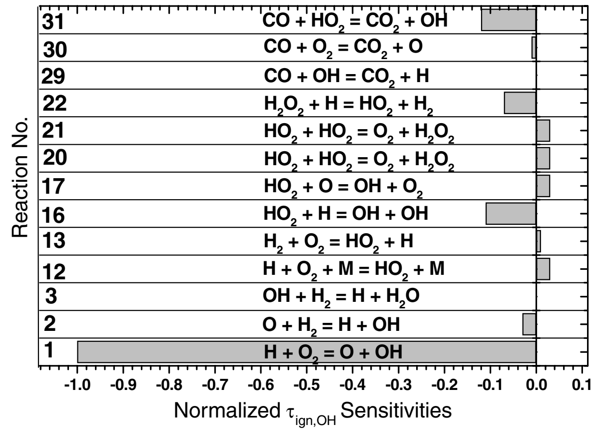

Fig. 12 Normalized ignition-delay-time sensitivities for mixture 1 (20% CO and 80% H_2) at $T = 1250$ K and $P = 1.05$ atm. Reaction 1 exhibits a strong ignition-delay-time sensitivity at lower temperatures and pressures.

important to study the ignition sensitivity of CO/H_2 mixtures for two opposite fuel compositions to determine which reactions dominate the ignition behavior when the mixture is either composed primarily of H_2 or CO. Subsequently, an ignition-delay-time sensitivity analysis was also applied to mixture 5 (90% CO and 10% H_2) to determine the effects of pressure on the sensitivity of the Davis mechanism reactions for both high (15 atm) and intermediate (2.5 atm) pressures at higher (1250 K) and intermediate temperatures (1050 K). In addition, a reaction-rate sensitivity analysis was performed on the Davis mechanism using the Senkin module of the Chemkin Collection [34] for the key radicals HO_2, H, and OH to complement the ignition-delay-time sensitivity analysis.

Because of the fact that the Davis mechanism predicted the experimental data accurately over the broad range of mixtures, temperatures, and pressures, it was chosen to be used in the sensitivity analysis. (However, because the other models qualitatively show the same behavior and use the same reactions, the sensitivity results should apply to them as well.) Using the OH concentration profile for each reaction i, the ignition delay time $\tau_{ign,OH}$ was calculated for reaction rates of $\frac{1}{2}k_i$ and $2k_i$. Subsequently, the ignition-delay-time sensitivity was defined as

$$(\tau|_{2k_i} - \tau|_{(1/2)k_i})/\tau|_{k_i} \qquad (4)$$

where a negative value for sensitivity indicates faster ignition. Results for each mixture and temperature were then normalized by the largest sensitivity value. Sensitivity values below 0.01 were neglected for mixture 1, and those below 0.02 were neglected for mixtures 5 and 6. Results for the τ_{ign} sensitivity are presented in Figs. 12–17.

It is apparent from Figs. 12–17 that reaction R1,

$$H + O_2 = O + OH$$

has the largest influence on the ignition delay time for the entire range of mixtures and test conditions herein. Although this important chain-branching reaction has a large influence on the overall system kinetics, other reactions also affect ignition characteristics, depending on temperature and level of hydrogen content.

For mixture 1 (20% CO and 80% H_2) at lower temperatures [900 K (Fig. 12)], there are three reactions with influential sensitivity values that are working to speed up ignition in addition to R1, each involving HO_2:

R16:

$$HO_2 + H = OH + OH$$

R22:

$$H_2O_2 + H = HO_2 + H_2$$

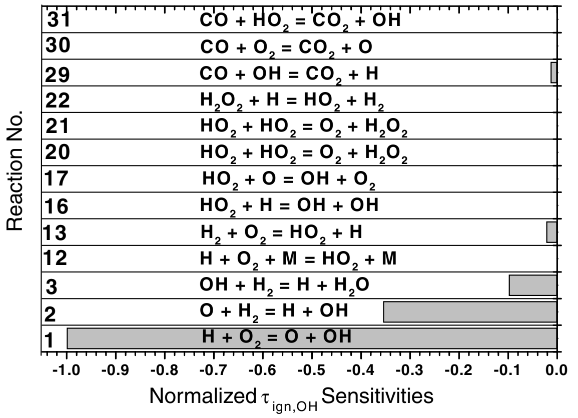

Fig. 13 Normalized ignition-delay-time sensitivities for mixture 1 (20% CO and 80%H_2) at $T = 900$ K and $P = 1.05$ atm. At higher temperatures the CO reactions are not as sensitive to changes in reaction rate; however, the H_2/O_2 chemistry is still dominant.

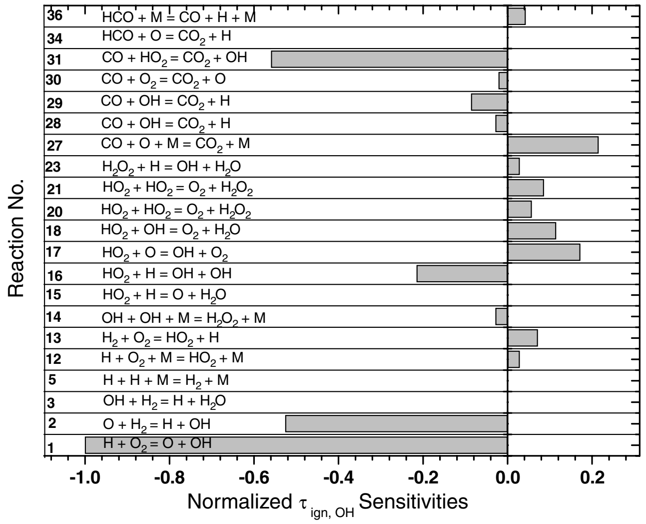

Fig. 14 Normalized ignition-delay-time sensitivities for mixture 6 (95% CO and 5%H_2) at $T = 900$ K and $P = 1.1$ atm. For mixtures containing reduced amounts of H_2, the CO chemistry is more sensitive to changes in reaction rate.

R31:

$$CO + HO_2 = CO_2 + OH$$

Although these three reactions have relatively large individual responses to changes in reaction rate and are the result of increased levels of HO_2 at lower temperatures, the ignition-delay-time plots indicate that τ_{ign} slows down at lower temperatures. The increase in ignition delay time at lower temperatures can be attributed to HO_2 recombination via R20/R21, the termination reaction R17, and HO_2 formation via R12:

R20/21:

$$HO_2 + HO_2 = O_2 + H_2O_2$$

R17:

$$HO_2 + O = OH + O_2$$

R12:

$$H + O_2 + M = HO_2 + M$$

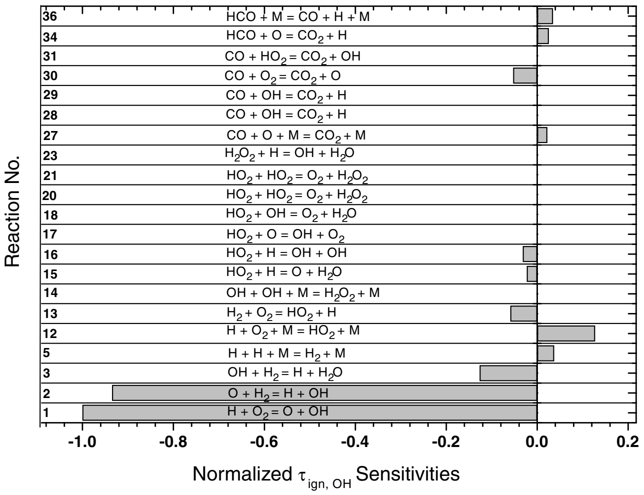

Fig. 15 Normalized ignition-delay-time sensitivities for mixture 6 (95% CO and 5%H_2) at $T = 1250$ K and $P = 1.1$ atm. Similar to mixture 1 at high temperature, the H_2/O_2 reactions that favor the production of OH radicals are most sensitive to changes in reaction rates.

Conversely, at higher temperature [1250 K (Fig. 13)] for the same mixture, the sensitivity analysis indicates that chain-propagating and chain-branching reactions are dominant (i.e., R1, R2, R13, and, to a lesser extent, R29), which all work to speed up ignition:

R2:

$$O + H_2 = H + OH$$

R3:

$$OH + H_2 = H + H_2O$$

R13:

$$H_2 + O_2 = HO_2 + H$$

R29:

$$CO + OH = CO_2 + H$$

Note that at the higher temperature for this mixture containing primarily hydrogen (mixture 1), the preceding four reactions have mostly minor impacts on ignition when compared with R1.

On the other hand, mixture 6, with only a marginal amount of H_2 (95% CO and 5% H_2), had many more reactions influencing ignition than mixture 1 (Fig. 14). Therefore, as mentioned earlier, instead of neglecting sensitivities below 0.01, those below 0.02 were neglected. Overall, the τ_{ign} sensitivity analysis for mixture 6 at lower temperature (900 K) indicates the same dominant H_2/O_2 reactions as the lower-temperature mixture 1 case described earlier. However, although the reactions were similar, mixture-6 reactions showed a much larger response to changes in reaction rate than mixture 1 (for example, R1 was by far the most sensitive reaction for mixture 1, with minimal changes in sensitivity for the other ignition-enhancing reactions R16 and R31). For mixture 6 at 900 K, R1, R2, R16, and R31 all had a significant impact on ignition. Most notably, the $CO + HO_2$ reaction (R31) becomes a primary ignition promoter at lower temperatures for higher levels of CO in the initial mixture.

Although the ignition-enhancing reactions had large sensitivity values, several key inhibiting reactions are also contributing to the slow ignition trend at lower temperatures. In fact, the reactions contributing most to the slowing down of ignition in this lower-temperature region include the HO_2-containing reactions R17, R18, and R20/R21 and the CO_2-formation reaction R27:

R18:

$$HO_2 + OH = O_2 + H_2O$$

R27:

$$CO + O + M = CO_2 + M$$

It should be noted that although the ignition kinetics are still dominated by the H_2-oxidation system, reactions involving CO become more important for this mostly CO-containing mixture (mixture 6) (for example, R27, R29, and R31) than was seen in the mixtures with more H_2.

The mixture-6 higher-temperature (1250 K) ignition-delay-time sensitivity results (Fig. 15) show a much weaker effect of HO_2- and CO-containing reactions, with large sensitivities for R1 and R2. Also, the sensitivity of reaction 31 is almost completely diminished and is replaced by the CO oxidation reaction R30:

$$CO + O_2 = CO_2 + OH$$

Additionally, the propagation reaction R3,

$$OH + H_2 = H + H_2O$$

becomes important at higher temperatures and contributes H radicals that then react with O_2 to form OH and O (i.e., R1). The large number of radicals that are formed during higher-temperature CO/H_2 combustion speeds up ignition.

To determine the effects of pressure on ignition-delay-time sensitivity, an analysis was conducted on mixture 5 (90%CO and $-10\%H_2$) for both 2.4 and 14.9 atm at 1050 K. A further analysis was completed to determine the effects of higher temperature (1250 K) and intermediate temperature (1050 K) at high pressure (14.9 atm). These results are presented in Figs. 16 and 17, respectively. Again, the two chain-branching reactions R1 and R2 are working to promote ignition. Although these two radical-producing reactions are working to promote and accelerate ignition, the most sensitive reaction for the intermediate-pressure range is R12. This reaction (R12) works to counteract the ignition-promoting reactions R1 and R2 and is actually slowing down ignition. For the conditions of this study, $M = N_2$ is the dominant collision partner because of the high level of N_2 in the mixture before and during the ignition process. For the high-pressure regime (14.9 atm), Fig. 16 shows many more sensitive reactions than for the 2.4-atm case. Again, R1 has a large sensitivity, as does R12. It is interesting to note, however, that R14,

$$OH + OH + M = H_2O_2 + M$$

has a small positive value for the 2.4-atm case, but then has a more significant negative sensitivity at higher pressure (14.9 atm). Also, within the high-pressure regime, the CO kinetics begin to have a greater influence on ignition. In particular, the reaction R31 promotes ignition, whereas for midpressure, there is little contribution from this step.

In addition to noting the key reactions in each pressure regime for the same temperature, it is also important to determine which reactions are most sensitive to changes in temperature for the same pressure. Figure 17 displays ignition-delay-time sensitivity results for mixture 5 (90%CO and $-10\%H_2$) for an average pressure of 14.9 atm at two temperatures: 1250 K and 1050 K. Again, R1 and R12 are the dominant reactions influencing ignition for both the higher- and lower-temperature cases. However, two reactions in particular are more important at lower temperatures: R14 and R31. In addition, there are three reactions with larger positive values of sensitivity at 1050 K than at 1250 K: R17, R18, and R27.

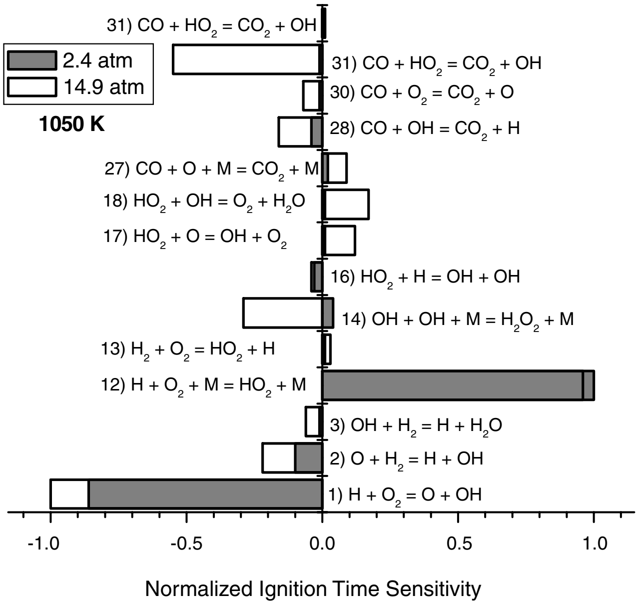

Fig. 16 Ignition-delay-time τ_{ign} sensitivity results for mixture 5 (90% CO and 10% H_2) for high and intermediate pressures and 1050 K.

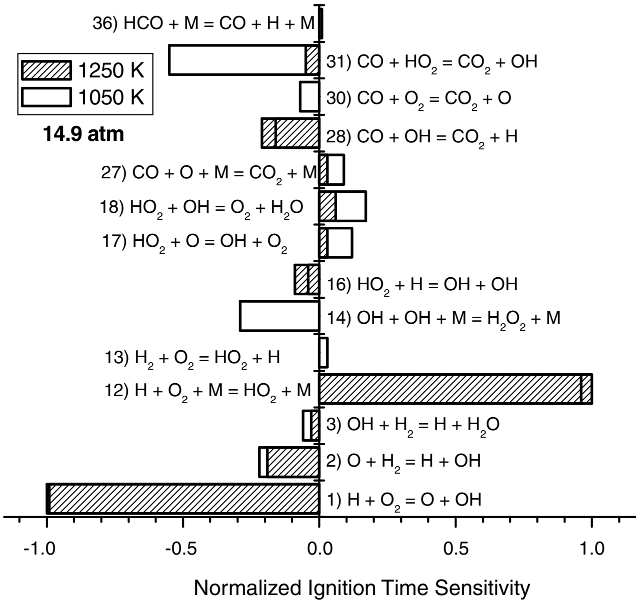

Fig. 17 Ignition-delay-time τ_{ign} sensitivity results for mixture 5 (90% CO and 10% H_2) for 1250 K and 1050 K at 14.9 atm.

The results from the high- and intermediate-pressure ignition-delay-time sensitivity analyses are similar to the 1-atm cases at both lower and higher temperatures. It can therefore be said that R1 is most critical for all pressure regimes ranging from 1 to 15 atm. In addition, high-pressure kinetics are similar to those at low temperatures. Although the H_2 kinetics play a dominant role, the CO kinetics should not be minimized in importance, especially at lower temperatures and higher pressures. It is the CO kinetics in particular that are the least studied, and reaction rates should be determined experimentally to improve CO/H_2 kinetics models (such as R31 and R27).

Reaction-rate sensitivity analyses were performed using Senkin for the key radicals HO_2, H, and OH to complement the ignition sensitivity analysis. The dominant reactions influencing radical buildup before ignition were found to be similar to the reactions promoting and inhibiting ignition mentioned earlier. For example, Fig. 18 shows a sensitivity plot for the H atom. Hydrogen radical formation is most sensitive to R1, R31, R14, and R28, whereas H-atom reduction is most sensitive to R12 and R27 at 1050 K and 14.9 atm.

Perhaps the most interesting feature of this reaction system is the large increase in ignition delay time when pressure is increased for the same temperature and mixture concentration. This is explained by the overwhelming importance of the third-body recombination reaction R12 in removing H atoms and, subsequently, delaying ignition at nearly all conditions of this study. The exception is the high-temperature, low-pressure, low-H_2 initial concentration

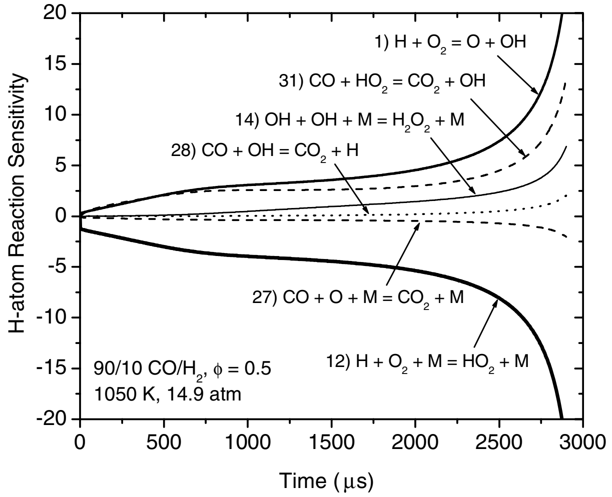

Fig. 18 Reaction-rate sensitivities for the H atom; mixture 5, 1050 K, 14.9 atm.

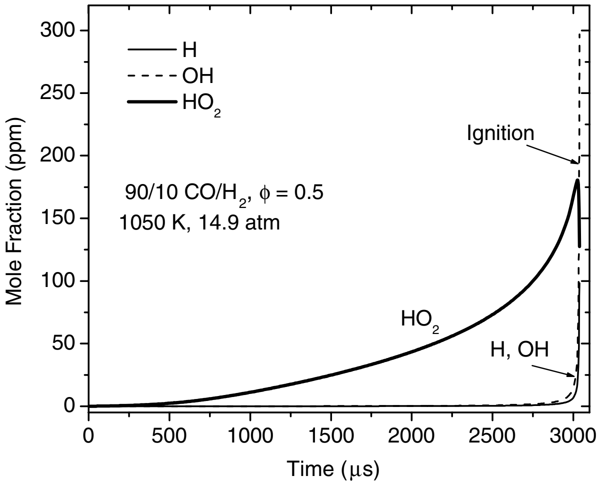

Fig. 19 Predicted time histories for HO_2, H, and OH showing dominance of HO_2 at early times. mixture 5, 1050 K, 14.9 atm.

mixture (2.4 atm and 95/5%CO/H_2 above 1100 K) in which other reactions become important. The ignition-delay-time behavior changes so dramatically with pressure because R12 is the only third-body reaction that plays an important role. The importance of R12 is shown in the τ_{ign} sensitivity calculations in Figs. 16 and 17 and in the H-atom reaction-sensitivity plot (Fig. 18). It is also demonstrated in the mole fraction time history of Fig. 19, which shows that H-atom concentrations (and, subsequently, OH concentrations) are suppressed as HO_2 is formed, until the very onset of ignition.

It is clear that R12 is extremely important in the ignition of syngas. However, there exists some uncertainty in its rate coefficient, particularly, with respect to different third-body collision species. Additional experiments have been performed to determine the rate of reaction 12 at different pressures and for both N_2 and Ar collision partners.

Discussion

Model Comparison

To better understand why the San Diego mechanism more accurately predicts the ignition-delay-time data for mixtures 5 (95/10%CO/H_2) and 6 (95/5%CO/H_2), all of the reactions and reaction rates within each of the five mechanisms were compared. In doing so, it was discovered that the San Diego mechanism was lacking the reaction $CO + O + M = CO_2 + M$, whereas all the other mechanisms included this recombination reaction. Although it is unknown why this particular reaction was not included in their mechanism, it is understood that the lack of the reaction within the mechanism is part of the reason that the mechanism more accurately predicts the ignition delay times for these two mixtures, indicating that perhaps its rate is too high in some or all of the mechanisms. In particular, because mixtures 5 and 6 contain the highest concentrations of CO for all the mixtures examined in this study, the absence of this reaction is more noticeable for these mixtures. In addition, without this reaction, more CO is converted to CO_2 through the $CO + HO_2$ propagation reaction, causing faster ignition than if the CO termination reaction were present (see Figs. 16 and 17).

Within the higher-pressure regime, it is apparent from Figs. 6–8 that there is a wide variation among the models: nearly a factor of 5 spread. Using the ignition-delay-time sensitivity analysis as a guide, several key reactions were examined to determine the source of disagreement at these high pressures. Upon further investigation, it was found that the probable cause of the variation in ignition delay times among the mechanisms at these conditions was again the CO chemistry. To understand how the CO chemistry was affecting the ignition-delay-time predictions of the models, the two models that were in worst agreement with the experimental data and with each other, the Sun and San Diego mechanisms, were analyzed.

As mentioned previously, the San Diego mechanism does not include the reaction $CO + O + M = CO_2 + M$, which results in an underprediction of the data at high pressure and intermediate temperature. This effect appears to be exaggerated at the higher pressure near 15 atm. Conversely, the Sun mechanism largely overpredicted the experimental data at the aforementioned conditions. A sensitivity analysis of this mechanism revealed that the same three H_2/O_2 reactions seen in Figs. 16 and 17 are most important; however, the reactions $CO + HO_2 = CO_2 + OH$ and $CO + O + M = CO_2 + M$ were largely sensitive, with a 0.41 normalized sensitivity. In contrast, calculations of the ignition-delay-time sensitivity of the Davis mechanism showed that the ignition times were much less sensitive to the $CO + O + M = CO_2 + M$ reaction, with only a 0.1 normalized sensitivity (Fig. 16). One conclusion that can be drawn here is that the reactions $CO + O + M = CO_2 + M$ and $CO + HO_2 = CO_2 + OH$ both need to be revisited to explain all of the data herein. Future versions of CO/H_2 mechanisms should include revisions of these two key CO reactions, and it seems that the best rates for the reactions are somewhat dependent on the separate mechanisms and the rates of the other important reactions within each.

Lowest-Temperature Data

As noted in the Results and Analysis section, the measured ignition delay times for a few of the data points at the lowest temperatures are noticeably shorter than that predicted by the kinetics mechanisms, as in Figs. 3, 4, and 9. At this time, it is not clear what the cause of this earlier ignition might be, although as mentioned earlier, there is a clear correlation between these few points and the occurrence of early combustion followed by the sudden appearance of a strong detonation wave. Nonetheless, others have seen similar effects in stoichiometric H_2/O_2 mixtures at elevated pressures and lower temperatures [35]. Various explanations such as nonideal effects behind the reflected shock wave have been put forth[¶] [35], but such explanations do not completely account for the discrepancies seen herein for the few data points so indicated. The possibility that the ignition for these few data points may have occurred in other than a zero-dimensional gas-phase kinetic situation could account for the discrepancy between the 0-D kinetics models and the experimentally observed ignition.[**] One observation by the present authors is that the early ignition at the lowest temperatures is highly repeatable and is therefore not a random event.

Experiments and analyses to determine the cause of the discrepancy between model and experiment at the lowest temperatures for the CO/H_2 (and H_2) system is a topic of further

---

[¶] Personal communication with F. L. Dryer and M. Chaos, 2007.

[**] Personal communication with F. L. Dryer and M. Chaos, 2007.

research in the authors' laboratory. The possibility that the faster ignition could be caused by impurities within the experiment is considered in more detail in the following section.

Effect of Impurities

It is well known from the literature that carbon monoxide ignition is quite sensitive to the presence of impurities (in particular, water vapor) [36,37]. It has been shown that H_2O can greatly accelerate the ignition process of CO/O_2/dilutent mixtures. Using the Davis kinetics mechanism, the effect of small levels of water vapor on CO ignition at the conditions of the present study was calculated. Figure 20 shows two ignition-time curves for a mixture of CO and air at $\phi = 0.5$ and 1 atm; one curve is for 100-ppm H_2O addition and the other is for 1000-ppm H_2O addition. Not shown on the graph is the case with zero water initially present, which would have a relatively semi-infinite ignition time and could not be shown on the same plot as the other curves. Given that the CO is difficult to ignite by itself at temperatures between 900 and 1250 K, the case with only 100-ppm water represents a dramatic decrease in the ignition delay time. Further acceleration of the ignition process is seen with 1000-ppm water addition, showing the increased sensitivity of ignition to increased levels of water vapor for the conditions indicated.

Of greater concern to the present study is whether CO/H_2 mixtures also show a high sensitivity to water addition. Therefore, a similar set of calculations was performed for the fuel blend with the least amount of H_2, or containing 95% CO by volume (mixture 6). The calculated ignition delay times at 1 atm for this mixture without initial water present are shown in Fig. 20. Also presented in Fig. 20 are the results with 100- and 1000-ppm H_2O present in the reactant mixture. The latter two curves are difficult to resolve in the graph, because they are identical to the curve with zero water vapor, indicating that mixture 6 with only 5% H_2 is kinetically insensitive to the presence of small levels of water vapor. This is an important conclusion, because it implies that syngas mixtures (and the results herein) are not sensitive to water at small levels. Care should be taken in extrapolating this result to much higher levels of water vapor. Because of the high third-body efficiency of the water molecule, ignition times in the regime in which R12 ($H + O_2 + M = HO_2 + M$) is important should actually lead to longer ignition delay times because of the inhibiting influence of R12 on ignition (see the preceding discussion).

Also of interest to the present study are impurities that might accelerate the ignition process by enhancing early radical production. For example, the authors have shown in recent experiments that small levels of silane can greatly accelerate the ignition of hydrogen mixtures and even counteract the inhibiting effect of R12 at lower temperatures [38]. To gauge the impact of impurities on the present experiments, a series of calculations was performed, again using the Davis mechanism. The impurities were modeled as an initial presence of H atoms, which was shown by Davidson and Hanson [39] to be a good model of the effect of radical impurities on the ignition process; they also pointed out the relatively high sensitivity of H_2-based mixtures to impurities. Figure 20 shows the results for a mostly CO fuel blend (mixture 6) with 1 ppm of H-atom impurities added. The effect of such an impurity is to decrease the ignition delay time rather uniformly across the temperature range of interest. Figure 21 shows the effect of impurities on a mixture with mostly H_2, or mixture 1 (80% H_2), in comparison with the ignition delay times of the pure mixture. As expected, impurities as modeled herein accelerate the ignition process, and an increase in the impurity level leads to even faster ignition.

From the results described in this section and in Figs. 20 and 21, one conclusion that can be drawn is that the effects of impurities, either H_2O or other, are not seen in the present experiments. This is an important point in light of the discrepancies seen between the model and experiment at the lowest temperatures and the fact that CO/H_2 kinetics are reasonably well known. For example, in Figs. 3 and 9, the agreement between model and data is excellent until about 950 K, below which the model overpredicts τ_{ign} by as much as an order of magnitude. Such a radical shift in the agreement does not correlate with the presence of impurities in the experiment, because if impurities were present in significant amounts, there would be a general acceleration of ignition and thus poor agreement between model and experiment over the entire temperature range, not just for temperatures below 950 K. Nothing changed in the experimental procedure to allow higher levels of impurities to be present in the lower-temperature cases than in any other experiment or mixture.

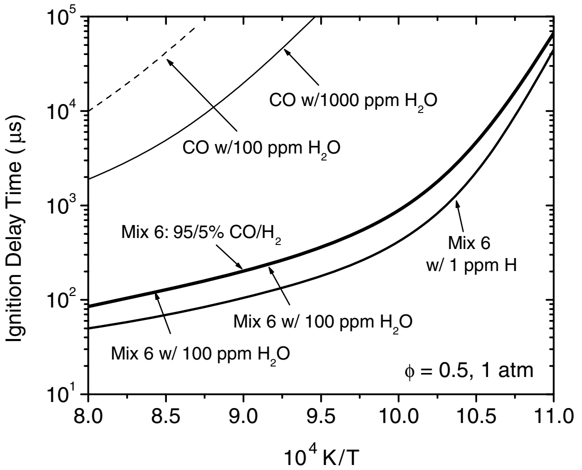

Fig. 20 **Effect of water and other impurities on a 100% CO and a 95%CO/5%H_2 fuel blend. Small levels of water vapor have a significant effect on pure CO ignition but no effect on the 95% CO blend.**

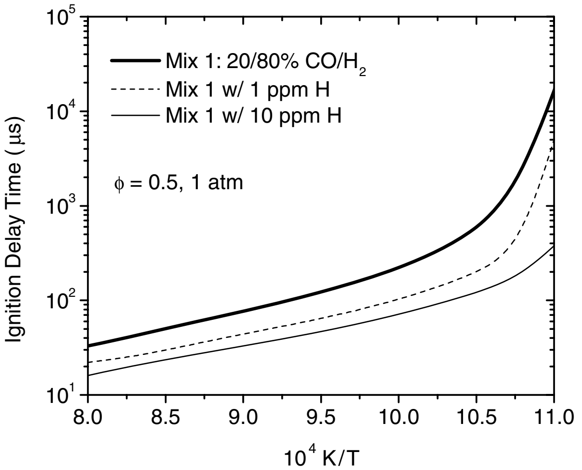

Fig. 21 **Calculated effect of impurities, modeled as H atoms, on a fuel blend with mostly hydrogen. The ignition delay time decreases with increasing levels of impurity, and the effects are evident at both lower and higher temperature.**

Conclusions

The kinetics of CO/H_2 oxidation are important for several reasons, ranging from improved CO/H_2 mechanisms for use in global hydrocarbon mechanisms to syngas applications in gas-turbine power-generation facilities. Although CO/H_2 oxidation has been studied for many years, the focus of the experimental research has not been on undiluted shock-tube ignition measurements and, therefore, there is a need for these data to validate current chemical kinetics mechanisms at engine conditions.

Ignition-delay-time measurements were conducted behind reflected shock waves for various fuel-lean CO/H_2/air mixtures. Reaction progress was monitored using OH* chemiluminescence for a range of temperatures ($890 \text{ K} < T < 1300 \text{ K}$) with pressures near 1, 2.5, and 15 atmospheres. The five chemical kinetics mechanisms used in this study were all in reasonable agreement with the experimental data, especially at higher temperatures, low to moderate pressures, and higher levels of hydrogen. In addition, they all qualitatively well modeled the change from low to high ignition activation energy that occurs near 1100 K at 1 atm. At lower temperatures and higher pressures, the models tended to overpredict the measured ignition delay time for a few points at the lowest temperature. These few points, however, can be linked to evidence of early reaction and subsequent strong detonation waves, setting them apart from the behavior of the other experimental data. The mechanisms indicate that the mixtures herein are insensitive to small levels of water impurity, and other impurities would not explain the discrepancies.

A τ_{ign} sensitivity analysis was conducted for three mixtures at low, intermediate, and high temperatures and at low and high pressures to determine the effects of different CO concentrations, temperature, and pressure on the overall system kinetics. It was found that although $H + O_2 = O + OH$ (R1) was the most sensitive reaction for all four cases (i.e., high and low CO concentration and high and low temperature), for lower-temperature (900 K) and higher-pressure (14.9 atm) ignition, the effects of this reaction are reduced by several reactions involving HO_2 and CO that ultimately slow down the ignition kinetics. For example, the ignition-promoting reaction $CO + HO_2 = CO_2 + OH$ becomes important at lower temperatures, but the HO_2 recombination and CO_2 formation reactions, among others, slow down ignition at 900 K. At higher temperatures, the ignition delay time is dominated by reactions from the hydrogen oxidation system for the entire range of initial H_2 content studied (5–80%). By comparing the different mechanisms, it was found that improvements can be made by focusing on the two CO_2-forming reactions $CO + O + M$ and $CO + HO_2$.

Acknowledgments

This work was supported primarily by a University Turbine Systems Research grant from the South Carolina Institute of Energy Studies, contract number 04-01-SR114, with Richard Wenglartz as the program monitor. Additional support came from The Aerospace Corporation and the National Science Foundation under grant CTS-0547159.

References

[1] Richards, G. A., McMillian, M. M., Gemmens, R. S., Rogers, W. A., and Cully, S. R., "Issues for Low-Emission, Fuel-Flexible Power Systems," *Progress in Energy and Combustion Science*, Vol. 27, No. 2, 2001, pp. 141–169.
doi:10.1016/S0360-1285(00)00019-8

[2] Sulzmann, K. G. P., Myers, B. F., and Bartle, E. R., "CO Oxidation, 1: Induction Period Preceding CO_2 Formation in Shock-Heated CO-O_2-Ar Mixtures," *Journal of Chemical Physics*, Vol. 42, No. 11, 1965, pp. 3969–3979.
doi:10.1063/1.1695869

[3] Myers, B. F., Sulzmann, K. G. P., and Bartle, E. R., "Oxidation of CO, 2: Influence of H_2 on the Induction Period Preceding Rapid CO_2 Formation in Shock-Heated CO-O_2-Ar Mixtures," *Journal of Chemical Physics*, Vol. 43, No. 4, 1965, pp. 1220–1228.
doi:10.1063/1.1696908

[4] Brabbs, T. A., Belles, F. E., and Brokaw, R. S., "Shock-Tube Measurements of Specific Reaction Rates in Branched-Chain H_2-CO-O_2 Systems," *Proceedings of the Combustion Institute*, Vol. 13, Aug. 1971, pp. 129–136.

[5] Gardiner, W. C., McFarland, M., Morinaga, K., Takeyama, T., and Walker, B. F., "Initiation Rate for Shock-Heated Hydrogen-Oxygen-Carbon Monoxide-Argon Mixtures as Determined by OH Induction Time Measurements," *Journal of Physical Chemistry*, Vol. 75, No. 10, 1971, pp. 1504–1509.
doi:10.1021/j100680a022

[6] Gardiner, W. C., Mallard, W. G., McFarland, M., Morinaga, K., Owen, J. H., Rawlins, W. T., Takeyama, T., and Walker, B. F., "Elementary Reaction Rates From Post-Induction-Period Profiles in Shock-Initiated Combustion," *Proceedings of the Combustion Institute*, Vol. 14, Aug. 1973, pp. 61–75.

[7] Dean, A. M., Steiner, D. C., and Wang, E. E., "A Shock Tube Study of the $H_2/O_2/CO/Ar$ and $H_2/N_2O/CO/Ar$ Systems: Measurement of the Rate Constant for $H + N_2O = N_2 + OH^*$," *Combustion and Flame*, Vol. 32, 1978, pp. 73–83.
doi:10.1016/0010-2180(78)90081-0

[8] Slack, M., and Grillo, A., "High Temperature Rate Coefficient Measurements of $CO + O$ Chemiluminescence," *Combustion and Flame*, Vol. 59, No. 2, 1985, pp. 189–196.
doi:10.1016/0010-2180(85)90024-0

[9] Cherian, M. A., Rhodes, P., Simpson, R. J., and Dixon-Lewis, G., "Kinetic Modelling of the Oxidation of Carbon Monoxide in Flames," *Proceedings of the Combustion Institute*, Vol. 18, Aug. 1981, pp. 385–396.

[10] Warnatz, J., "The Structure of Laminar Alkane-, Alkene-, and Acetylene Flames," *Proceedings of the Combustion Institute*, Vol. 18, Aug. 1981, pp. 369–384.

[11] Westbrook, C. K., and Dryer, F. L., "Chemical Kinetics and Modeling of Combustion Processes," *Proceedings of the Combustion Institute*, Vol. 18, Aug. 1981, pp. 749–764.

[12] Pitz, W. J., Westbrook, C. K., Proscia, W. M., and Dryer, F. L., "A Comprehensive Chemical Kinetic Reaction Mechanism for the Oxidation of N-Butane," *Proceedings of the Combustion Institute*, Vol. 20, Aug. 1984, pp. 831–843.

[13] Von Elbe, G., and Lewis, B., "Free-Radical Reactions in Glow and Explosion of Carbon Monoxide-Oxygen Mixtures," *Combustion and Flame*, Vol. 63, Nos. 1–2, 1986, pp. 135–150.
doi:10.1016/0010-2180(86)90116-1

[14] Maas, U., and Warnatz, J., "Ignition Processes in Carbon-Monoxide-Hydrogen-Oxygen Mixtures," *Proceedings of the Combustion Institute*, Vol. 22, Aug. 1988, pp. 1695–1704.

[15] Chung, S. H., and Williams, F. A., "Asymptotic Structure and Extinction of CO-H_2 Diffusion Flames with Reduced Kinetic Mechanisms," *Combustion and Flame*, Vol. 82, Nos. 3–4, 1990, pp. 389–410.
doi:10.1016/0010-2180(90)90010-O

[16] Yetter, R. A., Dryer, F. L., and Rabitz, H., "A Comprehensive Reaction Mechanism for Carbon Monoxide/Hydrogen/Oxygen Kinetics," *Combustion Science and Technology*, Vol. 79, Nos. 1–3, 1991, pp. 97–128.
doi:10.1080/00102209108951759

[17] Trevino, C., and Solorio, F., "Asymptotic Analysis of the High-Temperature Ignition of $CO/H_2/O_2$ Mixtures," *Combustion and Flame*, Vol. 86, No. 3, 1991, pp. 285–295.
doi:10.1016/0010-2180(91)90108-N

[18] Cho, S., and Niksa, S., "Elementary Reaction Models and Correlations for Burning Velocities of Multicomponent Organic Fuel Mixtures," *Combustion and Flame*, Vol. 101, No. 4, 1995, pp. 411–427.
doi:10.1016/0010-2180(95)00229-Y

[19] Mueller, M. A., Yetter, R. A., and Dryer, F. L., "Flow Reactor Studies and Kinetic Modeling of the $H_2/O_2/NO_x$ and $CO/H_2O/O_2/NO_x$ Reactions," *International Journal of Chemical Kinetics*, Vol. 31, No. 10, 1999, pp. 705–724.
doi:10.1002/(SICI)1097-4601(1999)31:10<705::AID-JCK4>3.0.CO;2-#

[20] Davis, S. G., Joshi, A. V., Wang, H., and Egolfopoulos, F., "An Optimized Kinetic Model of H_2/CO Combustion," *Proceedings of the Combustion Institute*, Vol. 30, Aug. 2005, pp. 1283–1292.
doi:10.1016/j.proci.2004.08.252

[21] Saxena, P., and Williams, F. A., "Testing a Small Detailed Chemical-Kinetic Mechanism for the Combustion of Hydrogen and Carbon Monoxide," *Combustion and Flame*, Vol. 145, Nos. 1–2, 2006, pp. 316–323.
doi:10.1016/j.combustflame.2005.10.004

[22] Li, J., Zhao, Z., Kazakov, A., Chaos, M., Dryer, F. L., and Scire, J. J., "A Comprehensive Kinetic Mechanism for CO, CH_2O, and CH_3OH Combustion," *International Journal of Chemical Kinetics*, Vol. 39, No. 3, 2007, pp. 109–136.
doi:10.1002/kin.20218

[23] Sun, H., Yang, S. I., Jomaas, J., and Law, C. K., "High-Pressure Laminar Flame Speeds and Kinetic Modeling of Carbon Monoxide/Hydrogen Combustion," *Proceedings of the Combustion Institute*, Vol. 31, Aug. 2007, pp. 439–446.
doi:10.1016/j.proci.2006.07.193.

[24] Petersen, E. L., Rickard, M. J. A., Crofton, M. W., Abbey, E. D., Traum, M. J., and Kalitan, D. M., "A Facility for Gas-and Condensed-Phase Measurements Behind Shock Waves," *Measurement Science and Technology*, Vol. 16, No. 9, 2005, pp. 1716–1729.
doi:10.1088/0957-0233/16/9/003

[25] Kee, R. J., Rupley, F. M., and Miller, J. A., "The Chemkin Thermodynamic Database," Sandia National Lab. Rept. SAND87-8251B, Albuquerque, NM, Mar. 1990.

[26] Vincenti, W. G., and Kruger, C. H., Jr., *Introduction to Physical Gas Dynamics*, Wiley, New York, 1965.

[27] Millikan, R. C., and White, D. R., "Systematics of Vibrational

Relaxation," *Journal of Chemical Physics*, Vol. 39, No. 12, 1963, pp. 3209–32113.
doi:10.1063/1.1734182

[28] Millikan, R. C., and White, D. R., "Vibrational Relaxation in Air," *AIAA Journal*, Vol. 2, No. 10, 1964, pp. 1844–1846.

[29] Dove, J. E., and Teitelbaum, H., "The Vibrational Relaxation of H_2, 1: Experimental Measurements of the Rate of Relaxation by H_2, He, Ne, Ar, and Kr," *Chemical Physics*, Vol. 6, No. 3, 1974, pp. 431–444.
doi:10.1016/0301-0104(74)85027-5

[30] Hooker, W. J., and Millikan, R. C., "Shock-Tube Study of Vibrational Relaxation in Carbon Monoxide for the Fundamental and First Overtone," *Journal of Chemical Physics*, Vol. 38, No. 1, 1963, pp. 214–219.
doi:10.1063/1.1733464

[31] Millikan, R. C., and White, D. R., "Vibrational Energy Exchange Between N_2 and CO. The Vibrational Relaxation of Nitrogen," *Journal of Chemical Physics*, Vol. 39, No. 1, 1963, pp. 98–101.
doi:10.1063/1.1734039

[32] Hall, J. M., and Petersen, E. L., "An Optimized Kinetics Model for OH Chemiluminescence at High Temperatures and Atmospheric Pressures," *International Journal of Chemical Kinetics*, Vol. 38, No. 12, 2006, pp. 714–724.
doi:10.1002/kin.20196

[33] GRI-Mech, Software Package, Ver. 3.0, Univ. of California, Berkeley, Berkeley, CA, available at http://www.me.berkeley.edu/gri-mech/.

[34] Chemkin Collection, Software Package, Ver. 4.0, Reaction Design, San Diego, CA, 2004.

[35] Martynenko, V. V., Penyaz'kov, O. G., Ragotner, K. A., and Shabunya, S. I., "High-Temperature Ignition of Hydrogen and Air at High Pressures Downstream of the Reflected Shock Wave," *Journal of Engineering Physics and Thermophysics*, Vol. 77, No. 4, 2004, pp. 785–793.
doi:10.1023/B:JOEP.0000045164.40205.6f

[36] Ahmed, S., and Back, M. H., "The Explosive Reaction of Carbon Monoxide and Oxygen at 973 and 1048 K," *International Journal of Chemical Kinetics*, Vol. 18, No. 7, 1986, pp. 801–817.
doi:10.1002/kin.550180707

[37] Pilling, M. J., and Noyes, R. M., "A Model for Explosions During Carbon Monoxide Oxidation," *International Journal of Chemical Kinetics*, Vol. 11, No. 8, 1979, pp. 821–841.
doi:10.1002/kin.550110803

[38] Petersen, E. L., Kalitan, D. M., and Rickard, M. J. A., "Reflected Shock Ignition of $SiH_4/H_2/O_2/Ar$ and $SiH_4/CH_4/O_2/Ar$ Mixtures," *Journal of Propulsion and Power*, Vol. 20, No. 4, 2004, pp. 665–674.

[39] Davidson, D. F., and Hanson, R. K., "Interpreting Shock Tube Ignition Data," *International Journal of Chemical Kinetics*, Vol. 36, No. 9, 2004, pp. 510–523.
doi:10.1002/kin.20024

C. Avedisian
Associate Editor